An actin-based viscoplastic lock ensures progressive body axis elongation

Alicia Lardennois[#1], **Gabriella Pásti**[#2], **Teresa Ferraro**[1], **Flora Llense**[1], **Pierre Mahou**[3], **Julien Pontabry**[2,4], **David Rodriguez**[2], **Samantha Kim**[2], **Shoichiro Ono**[5], **Emmanuel Beaurepaire**[3], **Christelle Gally**[2], **Michel Labouesse**[1,2,#]

[1]Sorbonne Université, Institut de Biologie Paris-Seine (IBPS), CNRS UMR7622, 9 Quai St-Bernard, 75005 Paris France

[2]Development and Stem Cells Department, IGBMC – CNRS UMR 7104/ INSERM U964/ Université de Strasbourg, 1 rue Laurent Fries, 67400 Illkirch, France

[3]Laboratoire d'Optique et Biosciences, Ecole Polytechnique, INSERM U1182 – CNRS/ UMR7645, 91128 Palaiseau cedex, France

[4]RS2D, 13 rue Vauban, 67450 Mundolsheim, France

[5]Departments of Pathology and Cell Biology, Winship Cancer Institute, Emory University School of Medicine, Atlanta, GA 30322, USA

[#] These authors contributed equally to this work.

Abstract

A key step in animal development is the process of body axis elongation, laying out the final form of the entire animal. This critically depends on polarized cell shape changes[1], which rely on the interplay between intrinsic forces generated by molecular motors[2–5], extrinsic forces due to adjacent cells pulling or pushing on the tissue[6–9], and mechanical resistance forces due to cell and tissue elasticity or friction[10–12]. Understanding how mechanical forces influence morphogenesis at the cellular and molecular level remains a critical challenge[2]. Recent work outlined that cell shape changes occur through small incremental steps[2,4,5,13], suggesting the existence of specific mechanisms to stabilize cell shapes and counteract cell elasticity. Here, we identify a spectrin-kinase-formin network required to stabilize embryo shape when repeated muscle contractions promote *C. elegans* embryo axis elongation. Its absence induces complete axis retraction due to damage of epidermal actin stress fibers. Modeling predicts that a mechanical viscoplastic deformation process can account for embryo shape stabilization. Molecular analysis suggests that the physical basis for viscoplasticity originates from the progressive shortening of epidermal microfilaments induced by muscle contractions and FHOD-1 formin activity. Our work thus identifies an essential molecular lock acting in a developmental ratchet-like process.

C. elegans provides a simple and integrated model to study the cellular impact of mechanical forces. Its embryonic elongation only relies on cell shape changes and includes two phases depending on tension and stiffness anisotropies in the epidermis[12], and beyond the 2-fold stage on muscle activity[8] (Fig. 1a; Supplementary material). Importantly, neither stage relies on pulsatile actomyosin flows[12], as observed in the early *C. elegans* zygote, or during *Drosophila* gastrulation and germband extension[2,4,5,13]. Because muscles are tightly mechanically coupled to the epidermis through epidermal hemidesmosomes[14], their contractions also displace the epidermis. This can be monitored by tracking the anterior-posterior displacement of muscle nuclei and the circumferentially oriented epidermal actin filaments (Fig. 1b–b'''). Importantly, all muscles do not contract simultaneously (X. Yang and M. Labouesse, unpublished). Hence, when some areas of the epidermis are longitudinally compressed (red line in Fig. 1c'), others are stretched (green line in Fig. 1c') before eventually relaxing (Fig. 1c–c''; Fig. S1). Importantly, we previously established that the tension generated by muscle activity triggers a mechanotransduction pathway in the epidermis, which promotes axis elongation[8].

The relaxation observed after each muscle contraction raises a conundrum: how can muscle activity power embryonic elongation from 100 μm to 200 μm within an hour if cell elasticity brings cells back to their initial length after each contraction (Fig. 1d). One simple hypothesis would be that some mechanism stabilizes the transient body deformations induced by muscle activity (Fig. 1d'), as was proposed for *Drosophila* gastrulation or germband extension in processes involving myosin II[5,15,16]. To uncover this mechanism, we focused on the kinase PAK-1, which lies at the crossroads of hemidesmosome remodelling[9] and actomyosin force regulation[17,18]. We first performed a feeding RNAi screen in a strong yet viable *pak-1* mutant, looking for enhancers of embryonic lethality and/or body morphology defects (Fig. 2a). This screen identified the gene *spc-1* encoding α-spectrin as a strong *pak-1* genetic enhancer leading to short hatchlings (58 μm on average), which were significantly shorter than *pak-1(tm403)* (178 μm) or *spc-1(RNAi)* (91 μm) hatchlings (Fig. 2b, Table S1). The study of this genetic interaction was further motivated by the identification of the central Src Homology 3 domain (SH3) of SPC-1 as an interactor of the N-terminal domain of PAK-1 in a yeast two-hybrid screen (Fig. 2c, Table S2). Both screens thus point to an interaction between SPC-1 and PAK-1.

To understand why *pak-1(tm403) spc-1(RNAi)* are shorter than *spc-1(RNAi)* embryos, we examined their elongation rate using DIC microscopy. Wild-type and *pak-1(tm403)* embryos initially elongated at the same rate, whereas *spc-1* defective embryos elongated slower and stopped around the 2-fold stage (100 μm) as previously described[19] (Fig. 2d). By contrast, *spc-1(ra409) pak-1(tm403)* and *spc-1(RNAi) pak-1(tm403)* embryos reached ≈65 μm at a slow rate, but then could not maintain their shape, retracting back to ≈50 μm, which neither *spc-1(ra409)* nor *pak-1(tm403)* embryos did (Fig. 2d, Movie 1). Two observations suggest that this phenotype is linked to muscle activity. First, *spc-1* knock-down in *git-1* or *pix-1* mutants, two other players involved in the same mechanotransduction pathway as PAK-1[9], also induced retraction (Fig. S2). Second, *spc-1(RNAi) pak-1(tm403)* embryos started to retract at the onset of active muscle contraction in control embryos (pink box in Fig. 2d). To directly prove this hypothesis, we abrogated muscle function in *spc-1(ra409) pak-1(tm403)*

embryos by knocking-down the kindlin homolog UNC-112[20]. Strikingly, *spc-1(ra409) pak-1(tm403)* embryos defective for *unc-112* no longer retracted (Fig. 2e; Movie 2). We conclude that the mechanical input provided by muscles to the epidermis induces the retraction phenotype observed in *spc-1 pak-1* double mutants.

The simplest interpretation of the retraction phenotype described above is that a cellular structure maintaining embryo shape fails to emerge or collapses in *spc-1 pak-1* double mutants once muscles become active. Two arguments lead us to consider that this structure corresponds to the actin cytoskeleton. First, SPC-1/α-spectrin and its binding partner SMA-1/ß-spectrin form an actin-binding hetero-tetramer colocalizing with actin[21] and partially with PAK-1 in epidermal cells (Fig. S3). Second and foremost, it has long been known that treating *C. elegans* embryos with the actin-depolymerizing drug cytochalasin-D induces a retraction phenotype very similar to that presented herein[22]. We thus characterized actin filaments by spinning-disk confocal imaging of a LifeAct::GFP probe[12]. Segmentation analysis of the fluorescence signal associated with actin filaments in the dorso-ventral epidermis (Fig. 3a–a''') revealed more discontinuity in *spc-1 pak-1* double deficient embryos (Fig. 3d–d''') compared to the control genotypes (Fig. 3a–c'''). Moreover, Fourier transform analysis indicated that their degree of anisotropy relative to the circumferential axis was abnormal (Fig. 3d''–d'''). Note that both phenotypes were visible mainly at mid elongation, i.e. after muscles become active (Fig. S4), suggesting that a well-structured actin network emerges too slowly in double mutants rather than it collapses.

Collectively, the results described so far, together with the retraction phenotype of cytochalasin-D treated embryos[22], suggest that the actin filament defects account for *spc-1 pak-1* embryo retraction, and further link muscle activity with these defects. Significantly, as the wild-type embryo lengthens, its circumference decreases by roughly 20% due to embryo volume conservation (Fig. S5) and thus, the length of actin filaments in dorso-ventral cells should decrease. Hence, we suggest that muscle activity normally promotes actin filament shortening, probably through sliding or shortening of filaments relative to each other after their bending (Fig. S1). We further suggest that SPC-1 and PAK-1 stabilize cell shape by maintaining actin bundle integrity. We could not define the shortening mechanism by spinning-disk microscopy, probably because each muscle contraction results in changes beyond the time and space resolution of the microscope. However, we suggest that it goes awry in the absence of SPC-1 and PAK-1, due to the lack of a capping or bundling activity (Fig. 4b–b').

To rationalize the role of muscles in the process of actin bundle shortening and stabilization, we described the *C. elegans* embryo as a Kelvin-Voigt material (a spring in parallel to a dashpot) submitted to forces acting in the epidermis and muscles (F_{epid} and $F_{muscles}$) (Fig. 4c equations-a and -b; Supplementary material). Note that F_{epid} is written as the product of an active force, F_{seam}, and a passive component resulting from actin bundle stiffness, a_{DV} (Supplementary material and ref. 11). Since muscle-defective mutants cannot elongate beyond the 2-fold stage, then F_{epid} can only extend embryos until that stage (due to the spring restoring force; Fig. S6a–a'). Simply adding the force $F_{muscles}$ should not trigger any further extension, because it oscillates between a positive and negative input (Fig. 1bc, Fig. S6b–b').

Recently, several studies have suggested that systems exposed to a stress can undergo a permanent rearrangement, which can be described as a plastic deformation[23] or as a change in the spring resting length[24,25]. Accordingly, we incorporated an increase of the spring resting length λ in the equations described above by writing that it changes by a factor β (Fig. 4c equation-c; Fig. 4d). Thereby, we could accurately predict the elongation pattern of wild-type embryos (Fig. 4f, Fig. S6d–d'; Supplementary material). Conversely, in *spc-1 pak-1* defective embryos, the continuing damage to actin filaments should reduce their stiffness (component a_{DV} in Fig. 4c equation-b), which we expressed by writing that it depends on a tearing factor γ (Fig. 4c equation-d, Fig. 4e); thereby, we could accurately predict their retraction pattern (Fig. 4f, Fig. S6e–e'). We thus propose that SPC-1/α-spectrin and PAK-1 regulate a process of mechanical plasticity in the physical sense. From a cellular standpoint, having a changing resting length means that body elasticity does not bring the embryo back to its initial shape upon muscle relaxation, enabling progressive lengthening.

To further define the molecular basis of viscoplasticity, we performed a small-scale RNAi screen to search for gene knockdowns inducing retraction of *spc-1(ra409)* embryos (Fig. 4g; Table S3). This screen identified the atypical formin FHOD-1 (Fig. 4h–i; Fig. S7, movie 3), which has previously been linked to actin dynamics in the epidermis[26]. We confirmed that *fhod-1(tm2363); spc-1(RNAi)* embryos also showed a penetrant retraction phenotype (Fig. 4h; Fig. S7). The identification of this specific formin was intriguing because vertebrate FHOD1 promotes actin capping and bundling rather than nucleation and elongation[27]. It thus raised the tantalizing possibility that FHOD-1 activity stabilizes the actin cytoskeleton while it gets remodeled under the influence of muscle activity during embryo circumference reduction. Furthermore, the genetic interaction suggests that FHOD-1 acts with SPC-1 and PAK-1. To examine this possibility, we tested whether FHOD-1 derivatives removing at least the C-terminal DAD domain, predicted to auto-inhibit formins[28], can rescue the retraction phenotype of *spc-1 pak-1* deficient embryos. Strikingly, after epidermis-specific expression of a form lacking the FH2 and DAD domains, transgenic *spc-1(RNAi) pak-1(tm403)* embryos did not retract and were significantly longer than non-transgenic siblings; rescue was better than with the full-length protein. By contrast, the DAD deleted form did not rescue and deletion of the FH1-FH2-DAD domains marginally rescued retraction, arguing that the FH2 F-actin nucleation domain is not necessary for rescue but that the FH1 is. Truncation of the C-terminal DAD domain or of the FH1-FH2-DAD domains marginally rescued retraction (Fig. 4j). Importantly, an FH2-DAD truncation in the mammalian FHOD1 still enables it to bundle actin[27], further strengthening the notion that FHOD-1 bundling activity is indeed required and providing a potential molecular basis for viscoplasticity. It also indicates that muscle-induced actin remodeling would primarily result from sliding and re-bundling (see Fig. 4a–a'). Furthermore, we conclude that the retraction of *spc-1 pak-1* deficient embryos mainly results from a lack of FHOD-1 activation.

Several factors could contribute to improperly regulate the activity of PAK-1 and FHOD-1. First, SPC-1 could help recruit FHOD-1 and PAK-1, since FHOD-1::GFP and PAK-1::GFP made small aggregates in SPC-1 defective embryos (Fig. S8). Second, we found that the cycles of actin filament displacement induced by muscle contractions were almost twice as short in *spc-1(RNAi) pak-1(tm403)* embryos compared to *pak-1(tm403)* and wild-type controls (3 sec against 5.7 sec; Fig. S9, Movie 4). These shorter muscle contractions might

still induce actin filament shortening but not give enough time for their stabilization. Third, PAK-1 might directly activate FHOD-1 downstream of the mechanotransduction pathway induced by muscles, since *git-1* and *pix-1* mutations combined with *spc-1* RNAi-knockdown also induced a retraction (see Fig. S2a–g).

Altogether, our data identify three proteins involved in stabilizing cell shapes in a system involving two mechanically interacting tissues submitted to repeated stress. We propose that the progressive shortening of actin filaments under the control of these factors mediates a cellular viscoplastic process promoting axis elongation. A similar spectrin/p21-activated kinase/FHOD1 system might operate in vertebrate tissues comprising an epithelial layer surrounded by a contractile layer, such as our internal organs. Interestingly, high FHOD1 expression correlates with poor prognosis of breast cancer patients[29]. Thus, a similar viscoplastic process might also influence the metastatic properties of tumor cells positioned next to contractile cells.

Supplementary Material

Refer to Web version on PubMed Central for supplementary material.

ACKNOWLEDGEMENTS

References

1. Tada M & Heisenberg CP Convergent extension: using collective cell migration and cell intercalation to shape embryos. Development 139, 3897–3904, doi:10.1242/dev.073007 (2012). [PubMed: 23048180]

2. Gilmour D, Rembold M & Leptin M From morphogen to morphogenesis and back. Nature 541, 311–320, doi:10.1038/nature21348 (2017). [PubMed: 28102269]

3. Keller R Developmental biology. Physical biology returns to morphogenesis. Science 338, 201–203, doi:10.1126/science.1230718 (2012). [PubMed: 23066066]

4. Martin AC, Kaschube M & Wieschaus EF Pulsed contractions of an actin-myosin network drive apical constriction. Nature 457, 495–499, doi:nature07522 [pii] 10.1038/nature07522 (2009). [PubMed: 19029882]

5. Rauzi M, Lenne PF & Lecuit T Planar polarized actomyosin contractile flows control epithelial junction remodelling. Nature 468, 1110–1114, doi:nature09566 [pii] 10.1038/nature09566 (2010). [PubMed: 21068726]

6. Collinet C, Rauzi M, Lenne PF & Lecuit T Local and tissue-scale forces drive oriented junction growth during tissue extension. Nat Cell Biol 17, 1247–1258, doi:10.1038/ncb3226 (2015). [PubMed: 26389664]

7. Desprat N, Supatto W, Pouille PA, Beaurepaire E & Farge E Tissue deformation modulates twist expression to determine anterior midgut differentiation in Drosophila embryos. Dev Cell 15, 470–477, doi:10.1016/j.devcel.2008.07.009 (2008). [PubMed: 18804441]

8. Lye CM et al. Mechanical Coupling between Endoderm Invagination and Axis Extension in Drosophila. PLoS Biol 13, e1002292, doi:10.1371/journal.pbio.1002292 (2015). [PubMed: 26544693]

9. Zhang H et al. A tension-induced mechanotransduction pathway promotes epithelial morphogenesis. Nature 471, 99–103, doi:10.1038/nature09765 (2011). [PubMed: 21368832]

10. Behrndt M et al. Forces driving epithelial spreading in zebrafish gastrulation. Science 338, 257–260, doi:10.1126/science.1224143 (2012). [PubMed: 23066079]

11. Dierkes K, Sumi A, Solon J & Salbreux G Spontaneous oscillations of elastic contractile materials with turnover. Phys Rev Lett 113, 148102, doi:10.1103/PhysRevLett.113.148102 (2014). [PubMed: 25325664]

12. Vuong-Brender TT, Ben Amar M, Pontabry J & Labouesse M The interplay of stiffness and force anisotropies drive embryo elongation. Elife 6, doi:10.7554/eLife.23866 (2017).

13. Munro E, Nance J & Priess JR Cortical flows powered by asymmetrical contraction transport PAR proteins to establish and maintain anterior-posterior polarity in the early C. elegans embryo. Developmental cell 7, 413–424, doi:10.1016/j.devcel.2004.08.001 (2004). [PubMed: 15363415]

14. Vuong-Brender TT, Yang X & Labouesse MC elegans Embryonic Morphogenesis. Curr Top Dev Biol 116, 597–616, doi:10.1016/bs.ctdb.2015.11.012 (2016). [PubMed: 26970644]

15. Simoes Sde M, Mainieri A & Zallen JA Rho GTPase and Shroom direct planar polarized actomyosin contractility during convergent extension. The Journal of cell biology 204, 575–589, doi:10.1083/jcb.201307070 (2014). [PubMed: 24535826]

16. Vasquez CG, Tworoger M & Martin AC Dynamic myosin phosphorylation regulates contractile pulses and tissue integrity during epithelial morphogenesis. The Journal of cell biology 206, 435–450, doi:10.1083/jcb.201402004 (2014). [PubMed: 25092658]

17. Gally C et al. Myosin II regulation during C. elegans embryonic elongation: LET-502/ROCK, MRCK-1 and PAK-1, three kinases with different roles. Development 136, 3109–3119, doi:10.1242/dev.039412 (2009). [PubMed: 19675126]

18. Vuong-Brender TTK, Suman SK & Labouesse M The apical ECM preserves embryonic integrity and distributes mechanical stress during morphogenesis. Development, doi:10.1242/dev.150383 (2017).

19. Norman KR & Moerman DG Alpha spectrin is essential for morphogenesis and body wall muscle formation in Caenorhabditis elegans. The Journal of cell biology 157, 665–677, doi:10.1083/jcb.200111051 (2002). [PubMed: 11994313]

20. Rogalski TM, Mullen GP, Gilbert MM, Williams BD & Moerman DG The UNC-112 gene in Caenorhabditis elegans encodes a novel component of cell-matrix adhesion structures required for integrin localization in the muscle cell membrane. The Journal of cell biology 150, 253–264 (2000). [PubMed: 10893272]

21. Praitis V, Ciccone E & Austin J SMA-1 spectrin has essential roles in epithelial cell sheet morphogenesis in C. elegans. Dev Biol 283, 157–170 (2005). [PubMed: 15890334]

22. Priess JR & Hirsh DI Caenorhabditis elegans morphogenesis: the role of the cytoskeleton in elongation of the embryo. Dev Biol 117, 156–173 (1986). [PubMed: 3743895]

23. Bonakdar N et al. Mechanical plasticity of cells. Nat Mater 15, 1090–1094, doi:10.1038/nmat4689 (2016). [PubMed: 27376682]

24. Doubrovinski K, Swan M, Polyakov O & Wieschaus EF Measurement of cortical elasticity in Drosophila melanogaster embryos using ferrofluids. Proc Natl Acad Sci U S A 114, 1051–1056, doi:10.1073/pnas.1616659114 (2017). [PubMed: 28096360]

25. Munoz JJ & Albo S Physiology-based model of cell viscoelasticity. Phys Rev E Stat Nonlin Soft Matter Phys 88, 012708, doi:10.1103/PhysRevE.88.012708 (2013). [PubMed: 23944493]

26. Vanneste CA, Pruyne D & Mains PE The role of the formin gene fhod-1 in C. elegans embryonic morphogenesis. Worm 2, e25040, doi:10.4161/worm.25040 (2013). [PubMed: 24778933]

27. Schonichen A et al. FHOD1 is a combined actin filament capping and bundling factor that selectively associates with actin arcs and stress fibers. J Cell Sci 126, 1891–1901, doi:10.1242/jcs.126706 (2013). [PubMed: 23444374]

28. Kuhn S & Geyer M Formins as effector proteins of Rho GTPases. Small GTPases 5, e29513, doi:10.4161/sgtp.29513 (2014). [PubMed: 24914801]

29. Jurmeister S et al. MicroRNA-200c represses migration and invasion of breast cancer cells by targeting actin-regulatory proteins FHOD1 and PPM1F. Mol Cell Biol 32, 633–651, doi:10.1128/MCB.06212-11 (2012). [PubMed: 22144583]

30. Vincent J in Structural Biomaterials: Third Edition 1–28 (Princeton University Press, 2012).
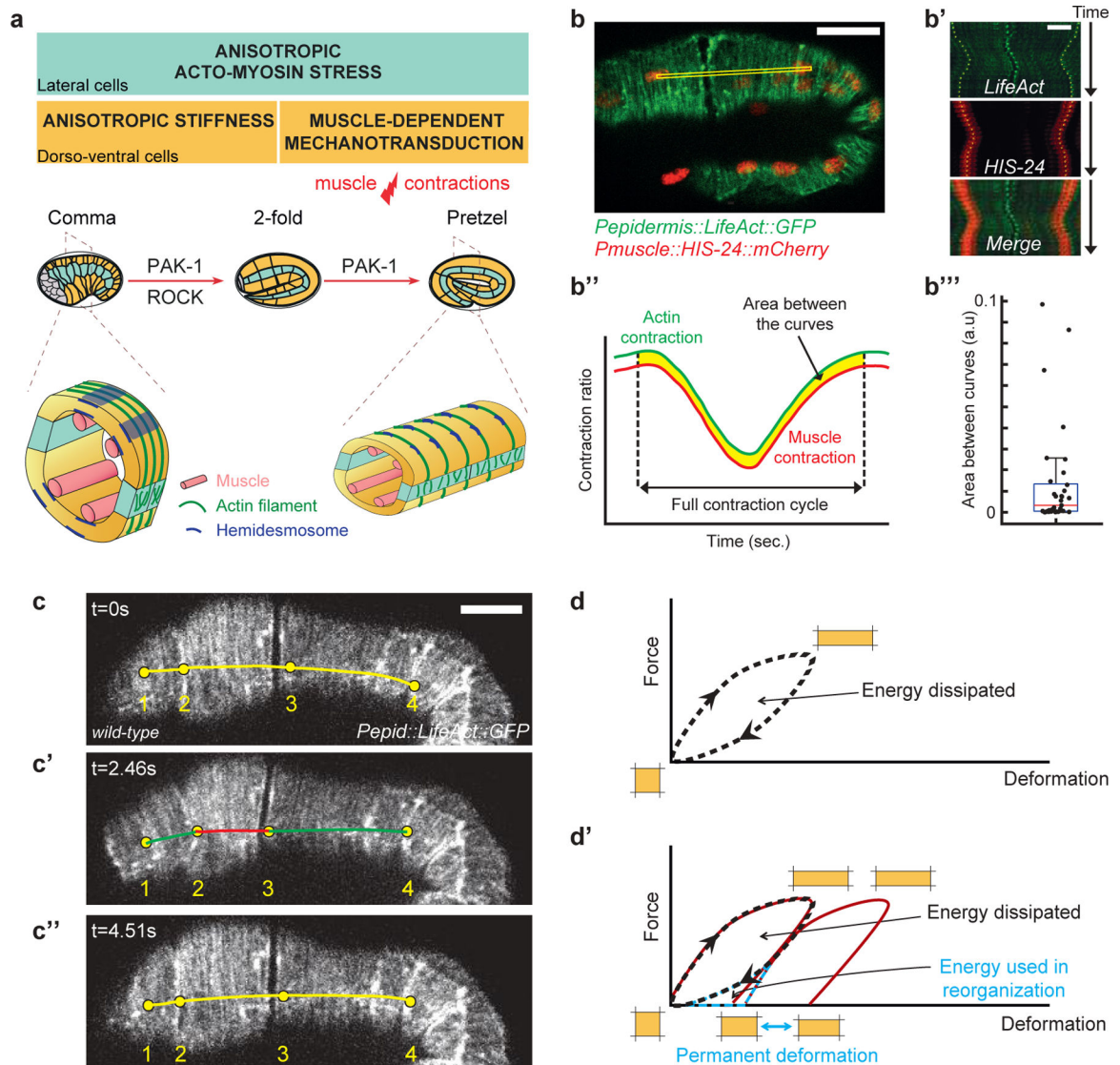
Figure 1: Muscle contractions deform the epidermis to their mechanical coupling

(a) *C. elegans* embryonic elongation from comma to 2-fold stages depends on a ROCK-promoted actomyosin force in seam cells (cyan) and actin-promoted stiffness in dorso-ventral cells (orange); elongation beyond the 2-fold stage requires repeated muscle contractions (red flash), which induce a PAK-1-dependent mechano-transduction pathway. Open cross-sections (bottom) show muscle positions. **(b-b''')** Epidermis actin filament (green) and muscle nucleus (red) tracking in a wild-type 2-fold embryo. **(b')** Kymographs from the yellow rectangle area **(b)** showing the concurrent displacement of epidermal actin and muscle nuclei. **(b'')** Resulting displacement curves; **(b''')** quantification of the area between them; its low value underlines the tight mechanical coupling between both tissues. Scale bar, 10 μm. **(c-c'')** A muscle contraction/relaxation cycle illustrating its local impact on epidermal actin filaments in a wild-type 2-fold embryo (timing in left corner). Yellow (relaxation), red (compression) green (stretching) distances between landmarks denoted 1–4: **(c)** [1–2], 7.8 μm; [2–3], 19.8 μm; [3–4], 24.6 μm. **(c')** [1–2], 9.4 μm; [2–3], 13.6 μm; [3–4],

26.2 μm. **(c'')** [1–2], 8.0 μm; [2–3], 19.2 μm; [3–4], 25.0 μm. In (**b-c**) the *Pepidermis* promoter is *Pdpy-7*. **(d)** Hysteresis graph of an idealized elastic material returning to its initial shape after deformation (top), or showing permanent deformation[30] (bottom).
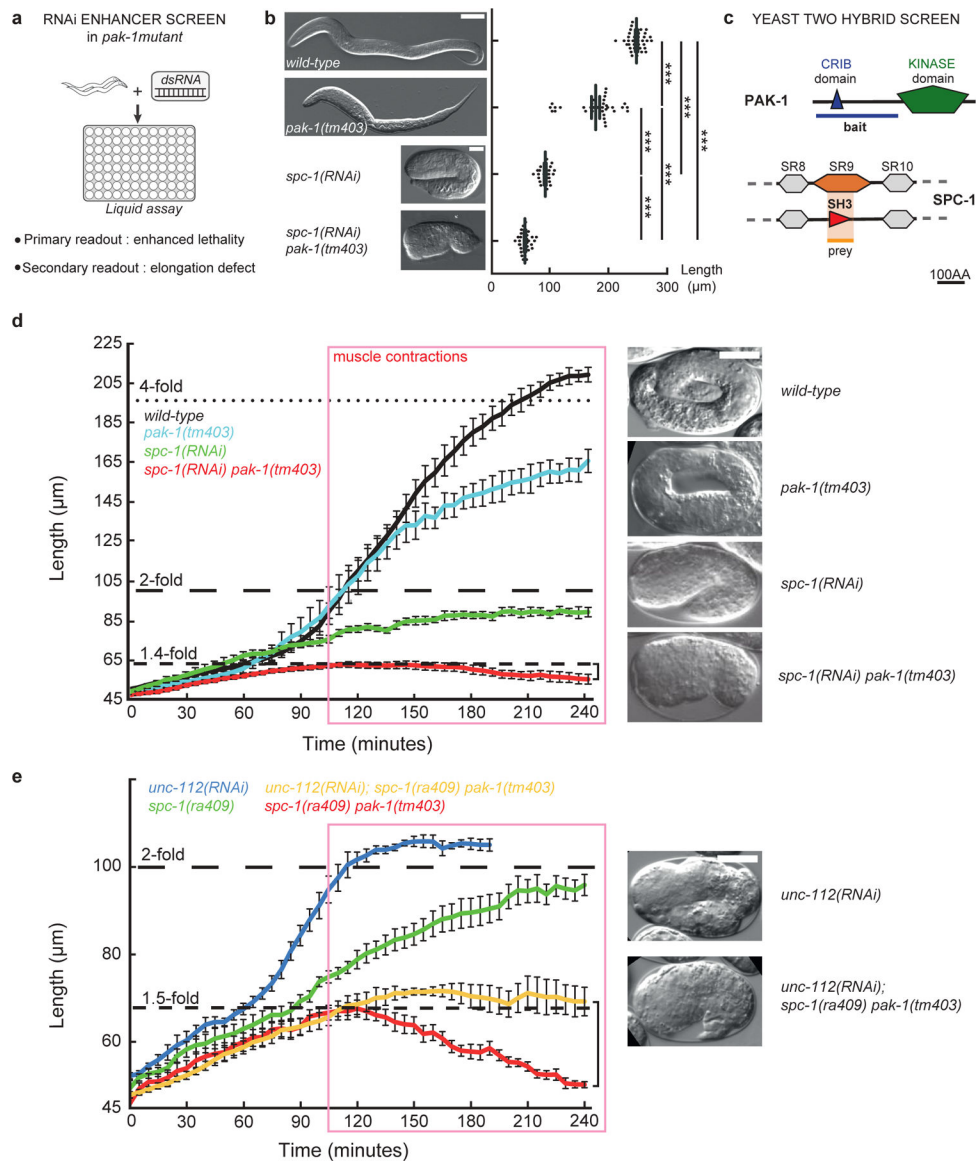
Figure 2: Loss of PAK-1 and SPC-1 triggers a muscle-dependent retraction of embryos
(a) RNAi screen in a *pak-1* mutant identified *spc-1* as an enhancer (Table S1). (b) DIC micrographs of newly hatched wild-type, *pak-1(tm403)* (scale bar: 10 μm), *spc-1(RNAi)* and *spc-1(RNAi) pak-1(tm403)* (scale bar: 25 μm). Quantification of L1 hatchling body length: wild-type (n=38); *pak-1(tm403) (n=32)*; *spc-1(RNAi)(n=26)*; *spc-1(RNAi) pak-1(tm40)* (n=36). (c) A yeast two-hybrid screen using the PAK-1 N-term domain as a bait identified the SPC-1 SH3 domain as a prey (orange background) (Table S2). (d) Elongation profiles and corresponding terminal phenotypes of wild-type (n=5), *pak-1(tm403)* (n=5), *spc-1(RNAi)* (n=8), *spc(RNAi) pak-1(tm403)* (n=8). (e) Elongation profiles in a muscle defective background. *unc-112(RNAi)* (n=5); *spc-1(RNAi)* (n=8); *unc-112(RNAi); pak-1(tm403) spc-1(ra409)* (n=5); *spc-1(RNAi) pak-1(tm403)* (n=8). Right bracket (**d, e**), extent of retraction for *spc-1(RNAi) pak-1(tm403)* embryos. Scale bars, 10 μm. Error bars, SEM.
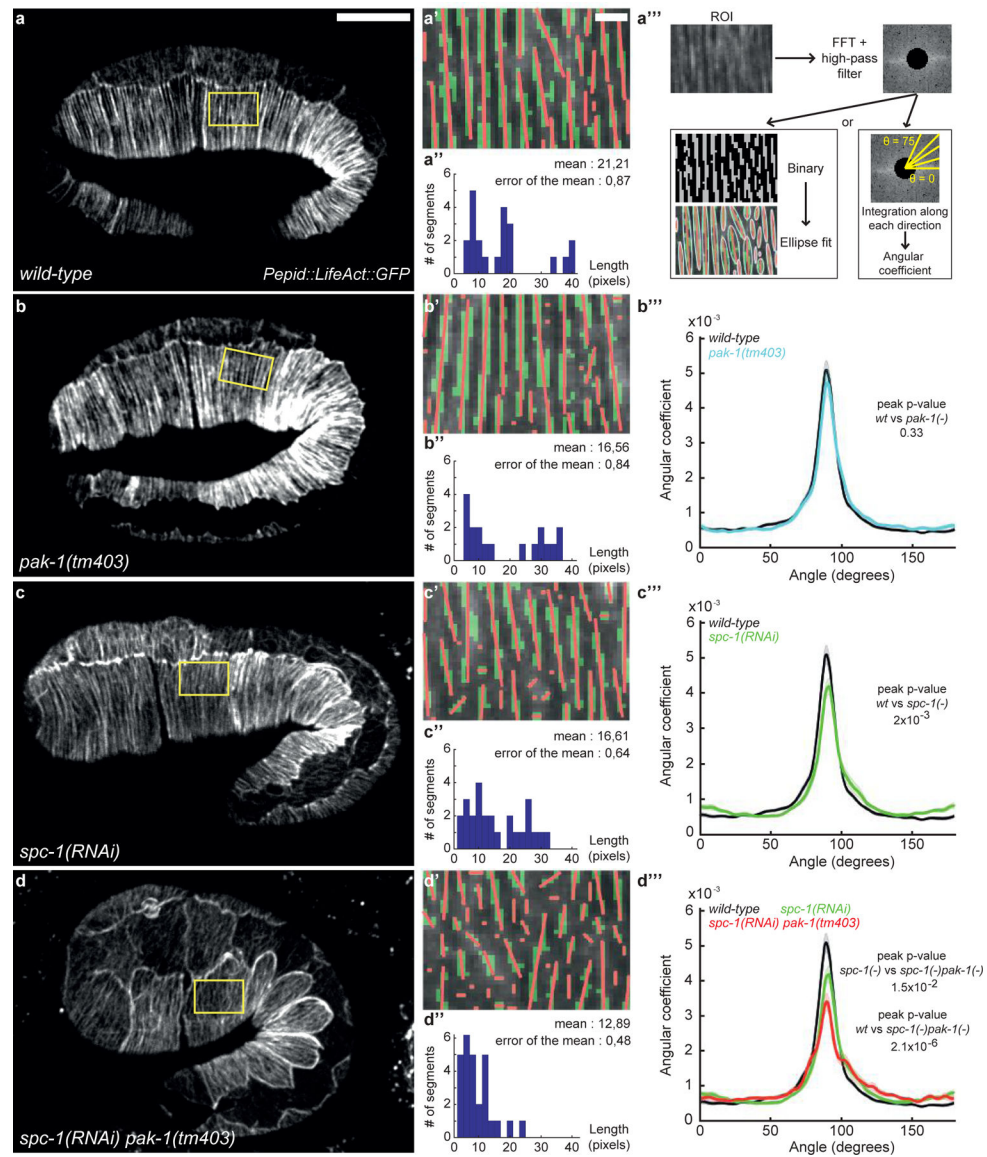
Figure 3: Actin filament defects in SPC-1 and PAK-1 defective embryos

(a-d) Epidermal actin filaments visualized with the *Pdpy-7::LifeAct::GFP* reporter construct in wild-type **(a-a''')**, *pak-1(tm403)* **(b-b''')**, *spc-1(RNAi)* **(c-c''')** and *spc-1(RNAi) pak-1(tm403)* **(d-d''')** embryos at mid-elongation (2-fold equivalent) stage. Yellow rectangle, region of interest (ROI). Scale bar, 10 μm. **(a'-d')** ROI after binarisation (green) and major axis detection (red), based on **(a''')** three steps of image treatment for continuity and orientation analysis. **(a''-d'')** Actin continuity: distribution of actin segments based on their length. Wild-type (n=16); *pak-1(tm403)* (n=21); *spc-1(RNAi)* (n=21); *spc-1(RNAi) pak-1(tm403)* (n=17*)* **(b'''-d''')** Actin filament orientation: the curves represent the number of actin filaments oriented perpendicular to the elongation axis (90° angle in wild-type) based on the Fast Fourier Transformation (FFT in a'''). Wild type (n=18); *pak-1(tm403)* (n=20); *spc-1(RNAi)* (n=18); *spc-1(RNAi) pak-1(tm403)* (n=18). Scale bars, 10 μm (c, d, e, f), or 1 μm (c', d', e', f'). P values, *<0,05; **<0,001; ***<0,0001; ns not significant.
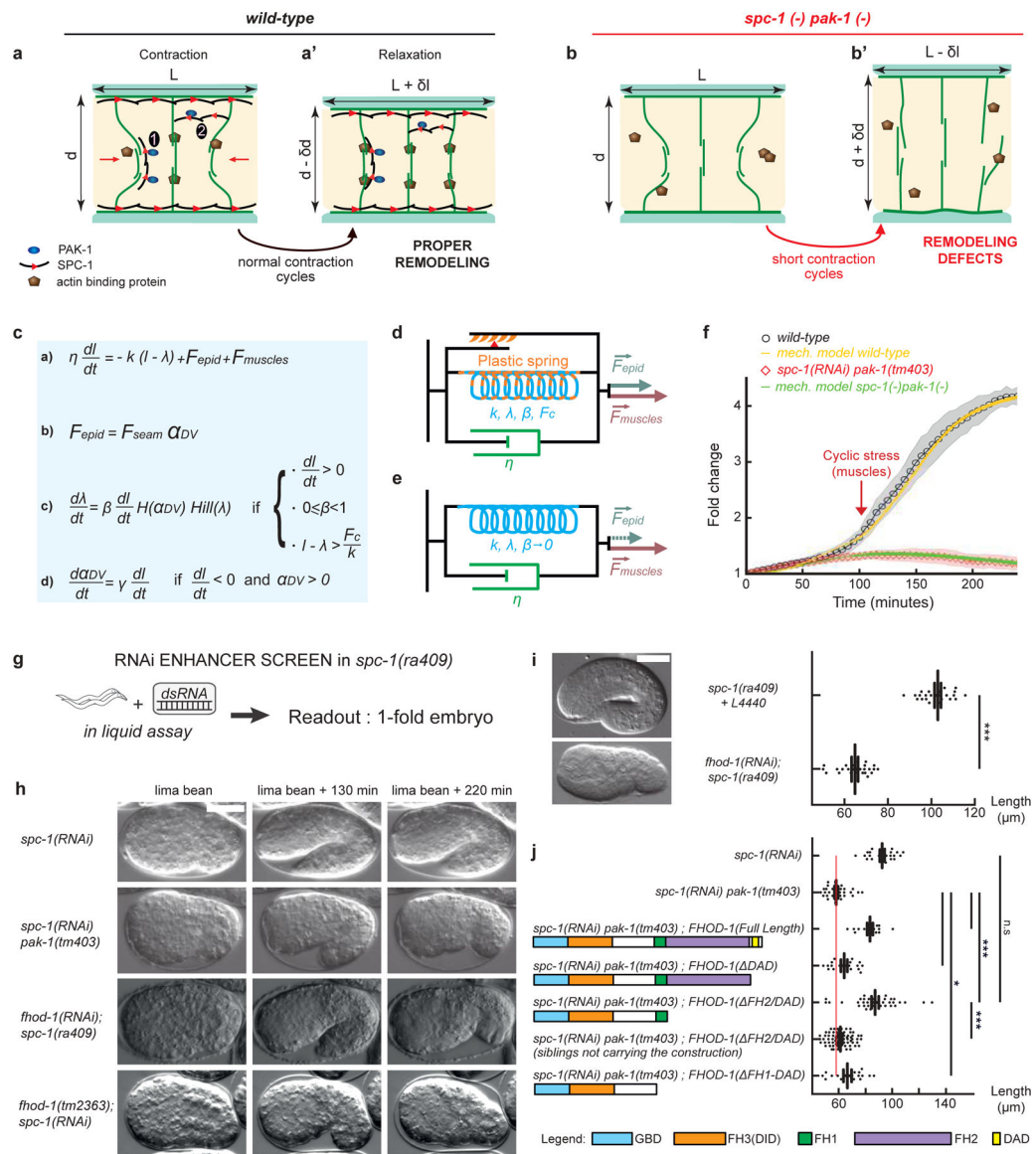
Figure 4: An actin-remodeling network providing mechanical plasticity ensures embryo elongation

(a-b') Cellular model of embryo elongation. (a-a') In control embryos, muscle contractions (red arrows) provoke actin filament shortening in the dorso-ventral epidermis, probably through sliding or shortening, followed by SPC-1/PAK-1-dependent actin stabilization. Whether spectrin is found along (scenario 1) or between (scenario 2) actin filaments is unknown (a). (b-b') In *spc-1 pak-1* deficient embryos, actin remodeling goes uncontrolled. (c-f) Viscoplastic mechanical model of embryo elongation. The embryo is represented as a Kelvin-Voigt solid (spring stiffness k, resting length λ, viscosity η) submitted to the forces F_{epid} and F_{muscle}. System equations for the model. (d) Wild-type case: an increasing resting length during stretching phases imparts mechanical plasticity. (e) *spc-1 pak-1* mutants: F_{epid} progressively decreases. (f) Comparison of experimental and predicted elongation curves taking the constitutive equations shown in (c). (g) A retraction screen in a *spc-1* mutant identifies *fhod-1*. (h) Snapshot at three time-points of *spc-1* deficient embryos in control,

pak-1 or *fhod-1* backgrounds; **(i)** terminal body length at hatching: *spc-1(ra409)* after feeding on L4440 control (n=21), or *fhod-1(RNAi)* (n=25) bacteria. **(j)** *Pdpy-7* driven epidermis expression of truncated FHOD-1 variants and terminal body length at hatching: *spc-1(RNAi)*(n=26); *spc-1(RNAi)pak-1(tm403)* no transgene (n=36), FHOD-1(full length) (n=16), FHOD-1(DAD) (n=17), FHOD-1(FH2-DAD) (n=38) and non-transgenic siblings (n=78), FHOD-1(FH1-FH2-DAD) (n=18). Scale bar, 15 μm. Error bars, SEM. P values: *<0,05; **<0,001; ***<0,0001; ns, not significant.